Journal of Power Sources 192 (2009) 708–713

Contents lists available at ScienceDirect

Journal of Power Sources

journal homepage: www.elsevier.com/locate/jpowsour

Short communication

A new low-temperature synthesis and electrochemical properties of LiV_3O_8 hydrate as cathode material for lithium-ion batteries

Yan Feng, Feng Hou, Yali Li*

Key Laboratory for Advanced Ceramics and Machining Technique of Chinese Education Ministry, School of Material Science and Engineering, Tianjin University, Tianjin 30072, PR China

ARTICLE INFO

Article history:
Received 30 October 2008
Accepted 20 February 2009
Available online 10 March 2009

Keywords:
LiV_3O_8
Cathode materials
Low-temperature synthesis
Lithium-ion battery

ABSTRACT

LiV_3O_8, synthesized from V_2O_5 and LiOH, by heating of a suspension of V_2O_5 in a LiOH solution at a low-temperature (100–200 °C), exhibits a high discharge capacity and excellent cyclic stability at a high current density as a cathode material of lithium-ion battery. The charge-discharge curve shows a maximum discharge capacity of 228.6 mAh g^{-1} at a current density of 150 mA g^{-1} (0.5 C rate) and the 100 cycles discharge capacity remains 215 mAh g^{-1}. X-ray diffraction indicates the low degree of crystallinity and expanding of inter-plane distance of the LiV_3O_8 phase, and scanning electronic microscopy reveals the formation of nano-domain structures in the products, which account for the enhanced electrochemical performance. In contrast, the LiV_3O_8 phase formed at a higher temperature (300 °C) consists of well-developed crystal phases, and coherently, results in a distinct reduction of discharge capacity with cycle numbers. Thus, an enhanced electrochemical performance has been achieved for LiV_3O_8 by the soft chemical method via a low-temperature heating process.

1. Introduction

Lithium vanadium oxides (LiV_3O_8) have been attracted as a promising cathode material for rechargeable lithium batteries because of their potentially high specific energy density, high working voltage and high discharge capacity, good chemical stability in air, ease of fabrication and low cost [1,2]. Although the LiV_3O_8 cathode in lithium batteries displays a high initial discharge capacity, the capacity decreases significantly with the cycle numbers [3,4], especially at a high discharge rate [5]. At a high current density > 100 mA g^{-1} (0.3C rate), the discharge capacity of LiV_3O_8 is low than 120 mAh g^{-1} after 50 charge-discharge cycles. A high discharge capacity and cycle stability are needed in high power applications.

Studies show that the electrochemical performance of LiV_3O_8 depends strongly on the preparation process. For improving the electrochemical performance of LiV_3O_8, different methods were developed to synthesize the materials, including high-temperature melting [6,7], sol–gel reactions [8,9], soft chemistry synthesis [4], hydrothermal synthesis [3,10], mechanical activation [11], microwave-assisted synthesis [12], flame spray pyrolysis synthesis [13] and freeze drying synthesis [5]. Of these methods, the soft chemistry route is relatively simple, involving only dispersion of precursors followed by heating. Liu et al. [14] prepared LiV_3O_8 from V_2O_5 and LiOH in their aqueous solution by heating at 480 °C for 10–12 h, and obtained an initial discharge capacity of 258 mAh g^{-1} measured at a low current density of 0.3 mA cm^{-2}. Guyomard and co-workers [8] prepared LiV_3O_8 from V_2O_5 and Li_2CO_3 by sol–gel method and heated at 650 °C for 10 h. The products show an initial discharge capacity of 210 mAh g^{-1} at ~90 mA g^{-1} current density. The cyclic stabilities of their materials decrease with the increasing of cycling. These studies involve heating of the reactants at a higher temperatures, between 300–600 °C [8,14]. It is known that the crystallinity of the phase has large effects on the electrochemical performance of LiV_3O_8 [5]. In particular, a low degree of crystallinity favors Li^+ intercalation and deintercalation leading to the improvement of discharge capacity [4].

In the present work, we synthesized LiV_3O_8 by heating the aqueous solution of V_2O_5 and LiOH at low-temperatures (100–300 °C). The products show an enhanced electrochemical performance and cyclic stabilities at a high current density in lithium batteries. XRD and SEM show the reduced degree of crystallinity and nano-domain structures of the LiV_3O_8 phases resulted from the low-temperature processing.

2. Experiment

V_2O_5 and $LiOH{\cdot}H_2O$ powders were dissolved in deionized water in a flask at the stoichiometric more ratio of 1.5:1 corresponding to LiV_3O_8. The solution was by magnetically stirred at 80 °C until

* Corresponding author. Tel.: +86 22 27403601; fax: +86 22 27402187.
E-mail address: liyali@tju.edu.cn (Y. Li).

0378-7753/$ – see front matter © 2009 Elsevier B.V. All rights reserved.
doi:10.1016/j.jpowsour.2009.02.079

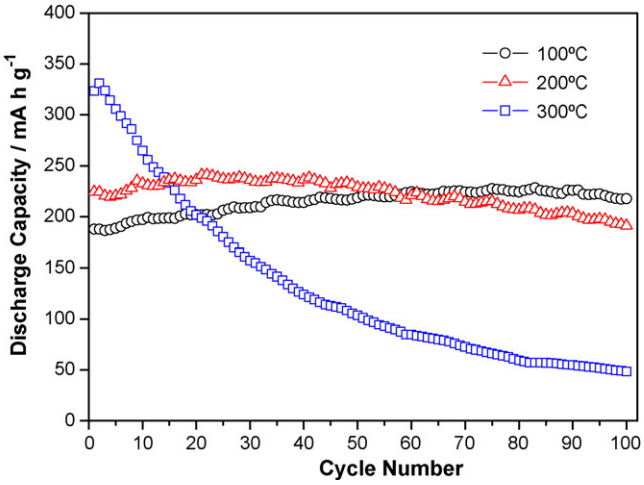

Fig. 1. The specific discharge capacities of LiV_3O_8 prepared at 100 °C, 200 °C and 300 °C. Current density: 150 mA g^{-1}; cut-offs: 4.0–1.8 V.

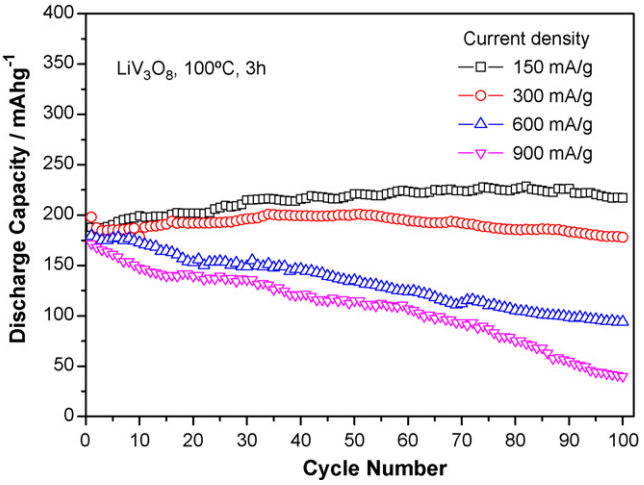

Fig. 2. The specific discharge capacities of LiV_3O_8 prepared at 100 °C at different current density.

the formation of a viscous orange gel after 0.5 h. The gel was heated at different temperature (100 °C, 200 °C and 300 °C) for 3 h. Orange powders were obtained and grounded by mortar to form fine powders of 200 meshes. The products were characterized using X-ray diffraction (XRD, Rigaku, D/MAX-2500 v/pc, CuKα) and scanning electron microscope (SEM, JEOL JSM-6700F).

Cathode electrodes were prepared by mixing the active material (LiV_3O_8, conductive additive (acetylene black) and binder (PTFE) in a weigh ratio of 85:10:5. The materials, as a cathode, were assembled into lithium batteries in an argon filled glove box, with the use of Celgard 2300 as a separator, Li foil counter and reference electrodes, and 1 mol dm^{-3} $LiPF_6$ in ethylene carbonate (EC), propylene carbonate (PC) and dimethyl carbonate (DMC) (1:1:1 by volume, Jinniu Corp., China) as electrolyte, to form laboratory-made coin-type cells (size: CR2032).

Cyclic voltammetry (CV) test were performed on a CHI 660C electrochemical workstation at a scan rate of 0.5 mV s^{-1} on the potential interval 1.6–4.2 V vs. Li^+/Li. The charge-discharge cycle tests were performed on a LAND 2001A battery testing system (Wuhan Jinnuo Corp.) in the potential range of 1.8–4.0 V vs. Li^+/Li. All the tests were performed at room temperature.

3. Results and discussion

The charge-discharge capacities of LiV_3O_8 synthesized at the different temperatures were measured at a high current density of 150 mA g^{-1}, as shown in Fig. 1. The 100 °C synthesized products show an initial capacity of 187.8 mAh g^{-1}, and the discharge capacity increases slightly with the cycle numbers attaining the maxima of 228.6 mAh g^{-1} at the 83 cycles, and then decreasing slowly. At 100 cycles, the capacity remains at 215 mAh g^{-1} keeping 94.05% of the maximum discharge capacity of 100 °C-LiV_3O_8 cathode. The 100 cycles discharge capacity is much higher than that of 175 mAh g^{-1} at the same current density (150 mA g^{-1}) for the LiV_3O_8 phase formed at a higher temperature through a traditional solid anneal reaction [15]. It is also higher than those of the 20–50 cycle capacities which are in the range of 180–200 mAh g^{-1} for LiV_3O_8 from freezing drying process [5], flame spray [13], and sol–gel derived LiV_3O_8 [16]. This shows the excellent cycle stability of our low-temperature synthesized LiV_3O_8 in lithium charge-discharge performance.

The stability of our LiV_3O_8 is still kept at a higher cycle numbers beyond 100 cycles, with the capacities being 187.9 mAh g^{-1} at 200 cycles, and 143.5 mAh g^{-1} at 300 cycles, which are 82% and 63% of

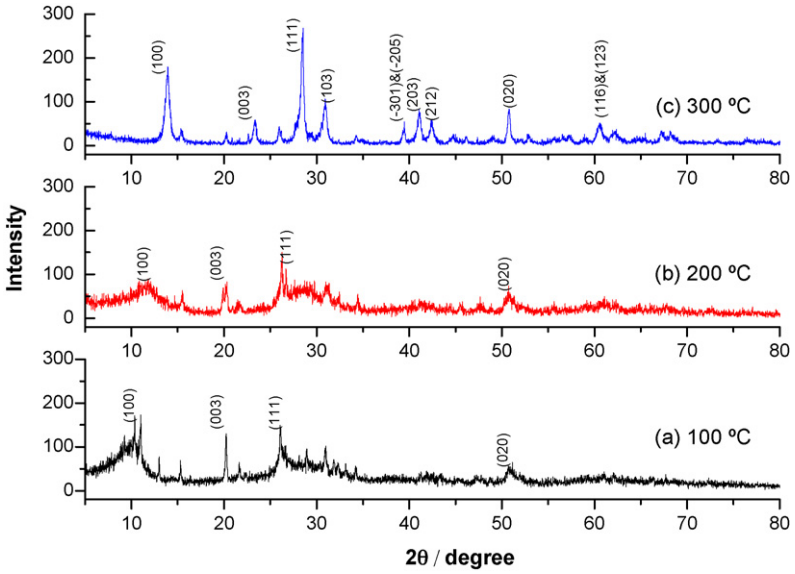

Fig. 3. XRD patterns of LiV_3O_8 prepared at different temperature (a) 100 °C; (b) 200 °C; (c) 300 °C.

the maximum discharge capacity, respectively. This value is higher than the present reports [15], indicating the excellent cycle stability of our 100 °C prepared LiV_3O_8 cathode.

The discharge capacities of LiV_3O_8 were measured at a higher discharge rate up to 900 mA g^{-1}, with the results shown in Fig. 2. The discharge capacity was 178 mAh g^{-1} at 300 mA g^{-1}, and 100 mAh g^{-1} at 600 mA g^{-1} after 100 charge-discharge cycles. At 900 mA g^{-1}, the discharge capacity was reduced to 50 mAh g^{-1} after 100 charge-discharge cycles. This indicates our LiV_3O_8 cathode material has good cycle stability and tolerable discharge capacity at $\leq$600 mA g^{-1} high rate charge-discharge, but > 600 mA g^{-1} high rate, this LiV_3O_8 cathode exhibits poor discharge capacity and cycle stability. These performances have not been reported detailedly.

The discharge capacities and cycle stabilities of LiV_3O_8 depend strongly on the processing temperatures. The products obtained at 100 °C and 200 °C both exhibit a high discharge capacity and good cycle stabilities, although they show a slight difference in the initial capacities, the 100 cycles discharge capacities and the changes of the capacities with the cycle numbers. The 200 °C-products have a maximum discharge capacity of 241.1 mAh g^{-1} attained at the 21 cycles, and the 100 cycle discharge capacity of 191.4 mAh g^{-1} being 79.89% of the maximum value. The 1–55 cycle capacity of the 200 °C-products is slightly higher than that of the 100 °C product,

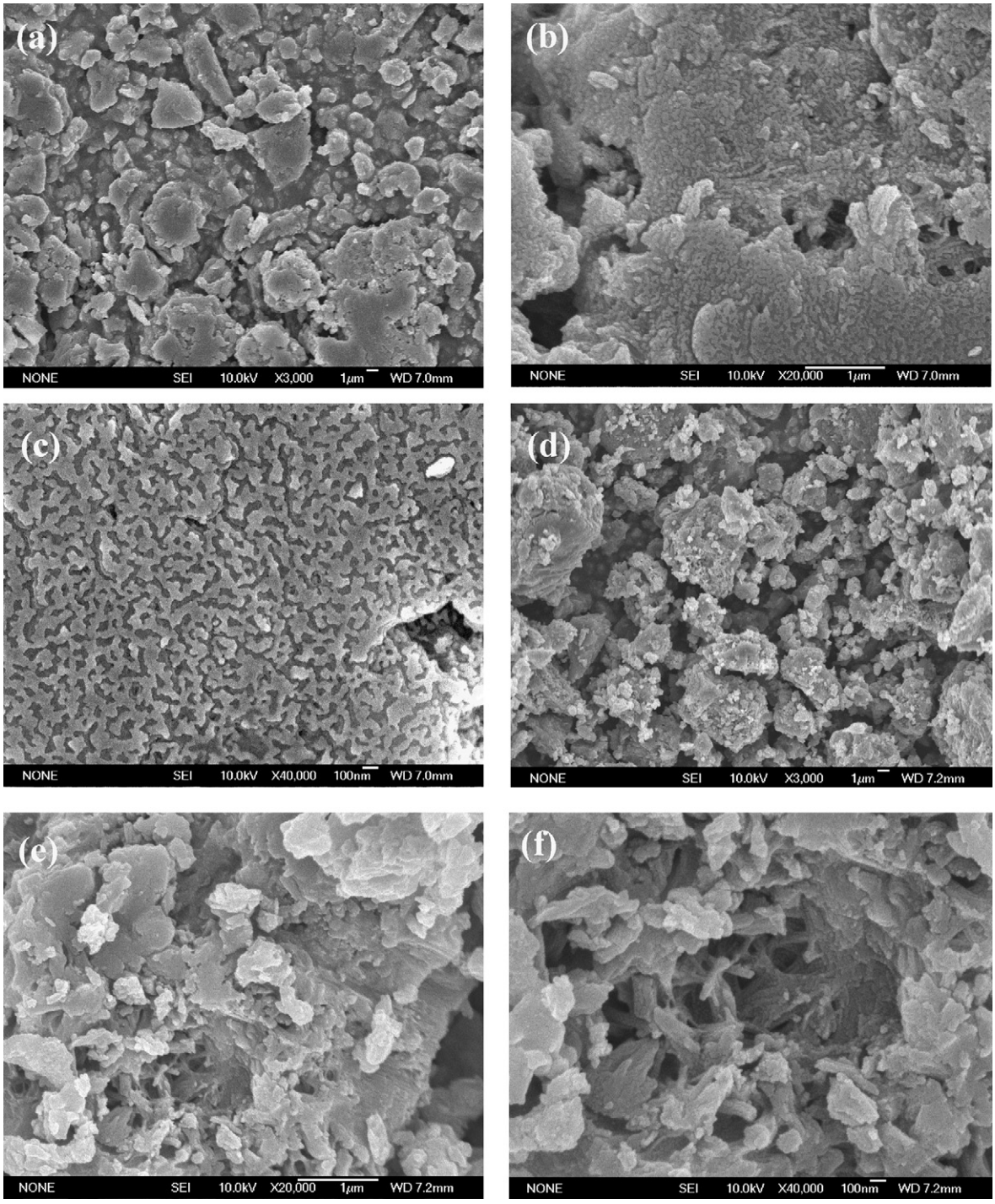

Fig. 4. SEM images of LiV_3O_8 prepared at (a, b, c) 100 °C; (d, e, f) 200 °C and (g, h, i) 300 °C.

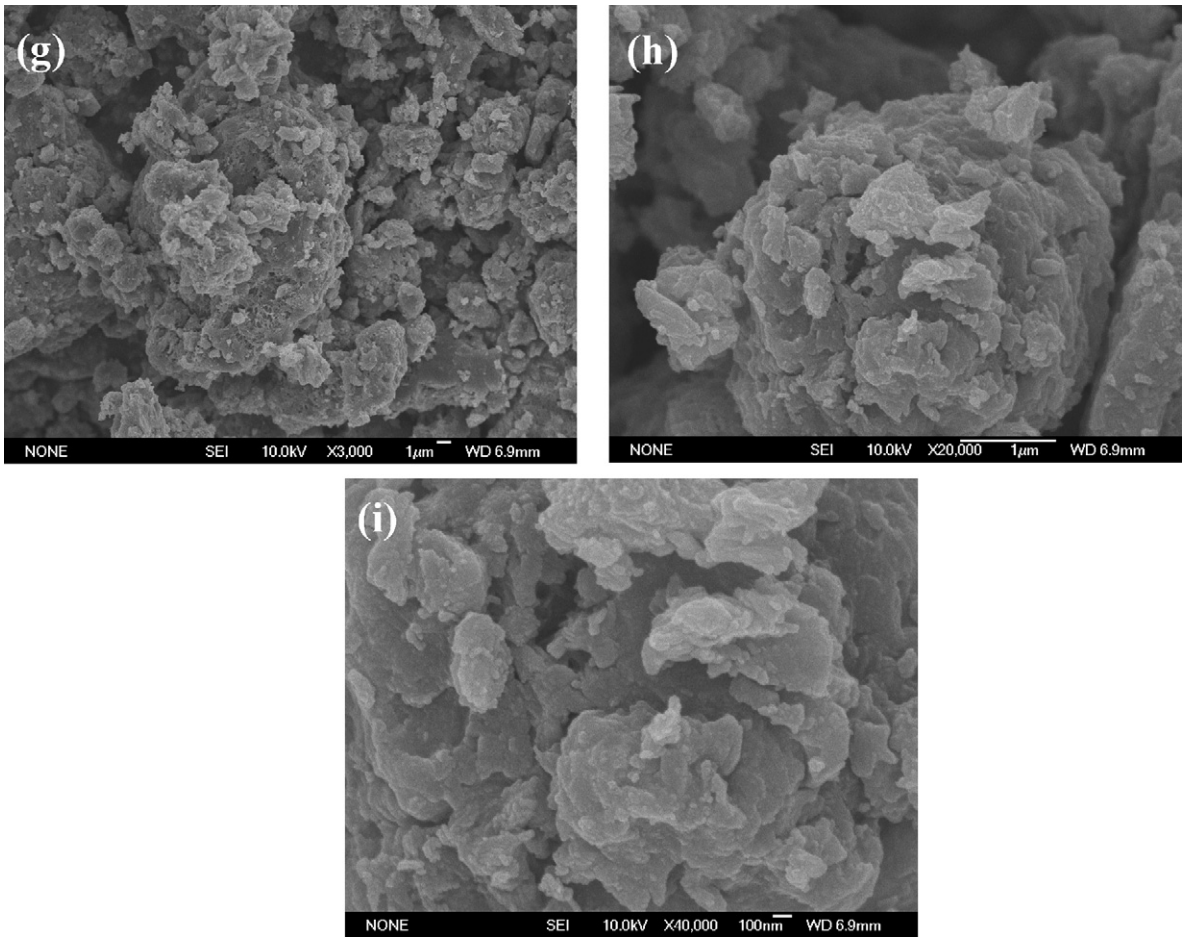

Fig. 4. (*Continued*).

and after 55 cycles, the discharge capacity reduces faster than the 100 °C product. Differently, the 300 °C products show a high initial capacity of 331 mAh g^{-1} attained at the second cycle, and a significant reduction of the discharge capacities down to 48.6 mAh g^{-1} after the 100 cycles of only 15% of the initial capacity. This indicates the poor discharge capacity of the products formed at the higher temperatures. Although the high preparation temperature decreases the discharge capacity of LiV_3O_8, it improves the initial discharge capacity.

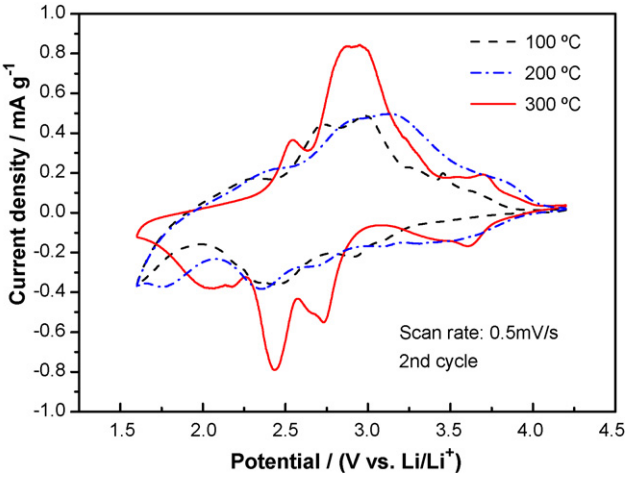

Fig. 5. CV curves (2nd cycle) of LiV_3O_8 cathode prepared at 100 °C, 200 °C and 300 °C.

The good cycle stability of the LiV_3O_8 formed at the lower temperatures (100–200 °C) attributes to their low degree of crystallinity, as identified by X-ray diffraction (XRD) (Fig. 3). The LiV_3O_8 products synthesized at the different temperatures shows the diffraction peaks of (1 0 0), (1 0 1), (0 0 2), (−1 1 1), all of which can be assigned to the crystalline phase of LiV_3O_8. Comparing to that synthesized at 300 °C, the intensities of these diffraction lines for the LiV_3O_8 formed at 100 °C and 200 °C are weaker and the peaks are broader, indicating the lower degree of crystallization. Moreover, the lattice parameter $d_{(1\,0\,0)}$ of the 100 °C products which is 8.540 Å, is much larger than that of 6.362 Å for the 300 °C product. This indicates the significant expanding of the inter-plane distance of LiV_3O_8 [17], as the result of a lower processing temperatures [17–19]. The $d_{(1\,0\,0)}$ = 8.540 Å for the 100 °C product is also much larger than that of 6.60–7.24 Å for the LiV_3O_8 products derived from a solid-reaction at 350 °C [18,19], indicating the significant changes of structures in the presently low-temperature processed LiV_3O_8. It is known that a low degree of crystallinity of LiV_3O_8 enhances the electrochemical performance of LiV_3O_8 [17–19]. The enhanced cycle stability of our materials attributes to the enlarged inter-plane spacing that provides larger interstitial and good channels for lithium transfer and diffusion [14]. The 200 °C products show similar phase structural behavior, which account for the similar discharging performance of the 200 °C products.

In contrast, the 300 °C products show well developed crystal phase of LiV_3O_8, as indicated by the distinctly increased intensity of the (1 0 0) peak (Fig. 3). This is accompanied by the decrease of the $d_{(1\,0\,0)}$ to 6.36 Å, as the result of the higher processing temperature. The rapid decreasing of discharge capacity with the cycle numbers

observed for this temperature produced products is thus associated to the narrowing of the (1 0 0) plane distance which was unfavorable for Li^+ to intercalate and deintercalate in the cathode [20].

Scanning electronic microscopy (SEM) shows different morphologies of the LiV_3O_8 formed at the different temperatures (Fig. 4). The 100 °C products consists of particulate phases of a flake-like morphology of 1–10 μm in sizes, which appear stacked in multi-layers (Fig. 4b). The higher magnification image reveals the formation of interconnected nano-domains of 50–200 nm covering the whole surfaces of the individual flask particles (Fig. 4c). Such nano-domain flask-morphologies have not been observed previously for LiV_3O_8. They are likely formed during the evaporation of water under heating at 100 °C. These flask-like nano-domian structures should contribute to the enhanced electrochemical properties of the 100 °C-formed products as it provides a larger higher surface area and good channels for lithium transfer, thus promoting the electrochemical reaction of charge-discharge cycle.

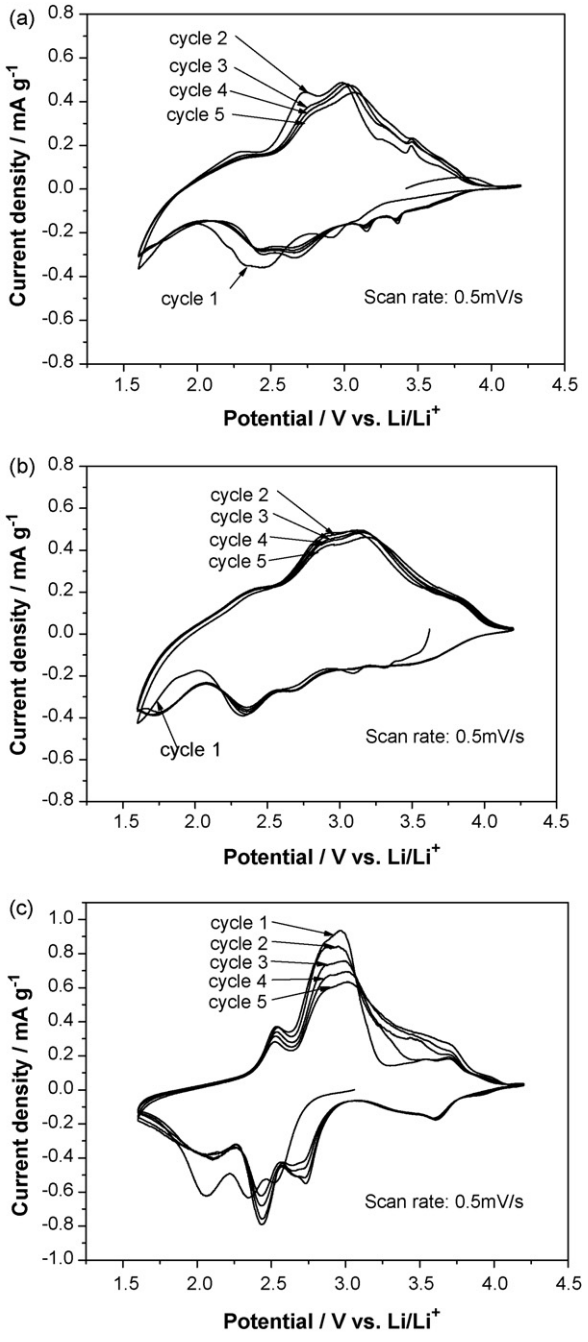

Fig. 6. CV curves (cycle 1–5) of as-prepared LiV_3O_8 cathode prepared at (a) 100 °C; (b) 200 °C; (c) 300 °C.

The 200 °C-formed appear the similar flask-like structures but of smaller sizes between 5–10 μm (Fig. 4d–f). Although there is absent of the nano-domains on the particle surface, some rod-like textures can be seen from the particles at a higher magnification (Fig. 4e, f). This indicates that the heating temperature controls the formation of the particle surface textures. Differently from the 100 and 200 °C-produced products, the 300 °C produced products appear as non-uniform particles, varying between of 5–20 μm in sizes (Fig. 4 g) and as blocked agglomerates. This is the direct result of the higher heating temperatures that led to rapid precipitation of particle phase and accelerate their growth and agglomeration. Such morphologies are less favored comparing to the nano-domain surface structures of the lower temperature synthesized products in respective of their electrochemical performance.

Finally, the charge–discharge behavior of the LiV_3O_8 products was followed by the CV profiles at a scan rate of 0.5 mV s^{-1} with a potential interval between 1.6–4.2 V in comparing to Li/Li^+ in 2nd cycle, as shown in Fig. 5. The 2nd cycle of LiV_3O_8 samples shows more than one reduction and oxidation peaks, displaying multiple charge and discharge plateaus [15]. The peaks for the 100 °C and 200 °C products are smoother and weaker than the 300 °C products, indicating less degree of transition in the lithium insertion process, thus leading to the better cycle stability [21]. Moreover, the reduction and oxidation peak intensity for 300 °C LiV_3O_8 is higher than the 100 °C and 200 °C products, suggesting the best discharge capacity attained at the first cycle and the fast kinetics for Li^+ intercalation/deintercalation in the electrode [22].

Fig. 6 is CV curves (cycle 1–5) of as-prepared LiV_3O_8 cathode prepared at (a) 100 °C; (b) 200 °C; (c) 300 °C. Except for the first cycle, the 2–5 cycles show much similar CV profiles for the 100 °C and 200 °C products, in contrast to that of the 300 °C products, indicating the excellent cyclic stabilities in accordance to that observed from the charge and discharge measurement (Fig. 4). The first cycle of CV profiles is rather different from the others. This is because during the first charge and discharge process, some structural modifications of the electrode materials have probably taken place. But with the cycling increased, the structure of electrode material becomes stable, leading to excellent charge–discharge stabilities to following cycling.

4. Conclusions

LiV_3O_8 synthesized from V_2O_5 and LiOH at a low-temperature remains 215 mAh g^{-1} after 100 cycle charge–dscharge at 150 mA g^{-1} current density and excellent cycle stabilities at high current rate, with discharge capacity maintained at 178 mAh g^{-1} after 100 cycles charge–discharge at 300 mA g^{-1} current density and 100 mAh g^{-1} after 100 cycles at 600 mA g^{-1} current density. Structural analysis indicates the low degree of crystallization of the low-temperature synthesized products and the formation of unique nanodomain structures, which account for the observed high electrochemical performance of the materials, as compared with the higher temperature synthesized materials. The good performance, along with the low synthesis temperature and the short heating time, make the process promising for high performance cathode for lithium-ion batteries.

Acknowledgements

This work was financially supported by the National Science Fund for Outstanding Young Scientists of China (No. 50625207) and sponsored by the National Post Doctoral Fund of China (No. 20070420695).

References

[1] A.L. Xie, C.A. Ma, L.B. Wang, Y.Q. Chu, Electrochim. Acta 52 (2007) 2945.
[2] J.X. Dai, F.Y. Li, Z.Q. Gao, K.S. Siow, J. Electrochem. Soc. 145 (1998) 3057–3062.
[3] H.W. Liu, H.M. Yang, T. Huang, Materials Sci. Eng. B 143 (2007) 60–63.
[4] Q.Y. Liu, H.W. Liu, X.W. Zhou, C.J. Cong, K.L. Zhang, Solid State Ionics 176 (2005) 1549–1554.
[5] O.A. Brylev, O.A. Shlyakhtin, A.V. Egorov, Y.D. Tretyakov, J. Power Sources 164 (2007) 868–873.
[6] A.M. Kannan, A. Manthiram, J. Power Sources 159 (2006) 1405–1408.
[7] A. Yu, N. Kumagai, Z.L. Liu, J.Y. Lee, J. Power Sources 74 (1998) 117–121.
[8] S. Jouanneau, A. Verbaere, S. Lascaud, D. Guyomard, Solid State Ionics 177 (2006) 311–315.
[9] J.G. Xie, J.X. Li, H. Zhan, Y.H. Zhou, Mater. Lett. 57 (2003) 2682–2687.
[10] H.Y. Xu, H. Wang, Z.Q. Song, Y.W. Wang, H. Yan, M. Yoshimura, Electrochim. Acta 49 (2004) 349–353.
[11] N. Kosova, E. Devyatkina, Solid State Ionics 172 (2004) 181–184.
[12] G. Yang, G. Wang, W.H. Hou, J. Phys. Chem. B 109 (2005) 11186–11196.
[13] T.J. Patey, S.H. Ng, R. Büchel, N. Tran, F. Krumeich, J. Wang, H.K. Liu, P. Novák, Electrochem. Solid-State Lett. 11 (2008) A46–A50.
[14] G.Q. Liu, N. Xu, C.L. Zeng, K. Yang, Mater. Res. Bull. 37 (2002) 727–733.
[15] M. Zhao, L.F. Jiao, H.T. Yuan, Y. Feng, M. Zhang, Solid State Ionics 178 (2007) 387.
[16] A. Deptula, M. Dubarry, A. Noret, J. Gaubicher, T. Olczk, W. Lada, Electrochem. Solid-State Lett. 9 (2006) A16–A18.
[17] V. Manev, A. Momchilov, A. Nassalevska, G. Pistoia, M. Pasquali, J. Power Sources 54 (1995) 501.
[18] A.S. Yu, N. Kumagai, Z.L. Liu, J.Y. Lee, J. Power Sources 74 (1998) 117–121.
[19] N. Kumagai, A.S. Yu, J. Electrochem. Soc. 144 (1997) 830–835.
[20] G.D. Liu, C.L. Zeng, K. Yang, Electrochim. Acta 47 (2002) 3239–3243.
[21] L. Liu, L.F. Jiao, J.L. Sun, M. Zhao, Y.H. Zhang, H.T. Yuan, Y.M. Wang, Solid State Ionics 178 (2008) 1756.
[22] C.Q. Feng, L.F. Huang, Z.P. Guo, J.Z. Wang, H.K. Liu, J. Power Sources 174 (2007) 548–551.